J|A|C|S COMMUNICATIONS

Published on Web 02/16/2009

Nonsurfactant Supramolecular Synthesis of Ordered Mesoporous Silica

Rambabu Atluri,[‡] Niklas Hedin,[†] and Alfonso E. Garcia-Bennett*[,‡]

Nanotechnology and Functional Materials, Department of Engineering Sciences, The Ångström Laboratory, Uppsala University, Box 534, SE-751 21 Uppsala, Sweden, and Materials Chemistry Research Group, Department of Physical, Inorganic and Structural Chemistry, Arrhenius Laboratory, Stockholm University, SE-106 91 Stockholm, Sweden

Received December 10, 2008; E-mail: alfonso.garcia@angstrom.uu.se

Hoogsteen-bonded tetrads and pentamers are formed by a large variety of organic molecules through H-donor and -acceptor groups, capable of inducing self-organization to form columnar and hexagonal mesophases. The biological importance of such macromolecular structures is exemplified by (1) the assembly of guanosine rich groups of telomere units with implications for chromosomal replication[1] and (2) folate derivatives, studied for the development of anticancer agents as increased folate receptors in tumor cells have led to several strategies for targeted drug delivery and treatment.[2−4] Folic acid is composed of a pterin group, chemically and structurally similar to guanine, conjugated to the L-glutamate moiety via a *p*-amino benzoic acid (Scheme 1a). Our aim has been to develop a reservoir delivery vehicle for sustained release of folic acid in one synthesis step and, at the same time, provide a novel synthetic route for ordered mesoporous materials without the use of amphiphilic surfactants or micellar species. To the best of our knowledge this is the first report of the formation of mesoporous materials without reliance on the formation of micelles.

Mesoporous silicate materials[5] have undergone extensive research since their discovery focusing on their synthetic control as well as their structural and compositional diversity.[6−8] Ordered porosity in the range 2−30 nm is accessible with narrow pore size distributions through carefully selected surfactant systems including polymeric, cationic, and anionic surfactants and mixtures of these.[9] The control of particle size, of great importance for the many emerging applications, has been investigated leading to the development of processing methods capable of tailoring both particle size and shape.[10−14]

In our preparation, we rely on the self-organization of pterin groups, stabilized through hydrogen bonding, exposing their glutamate moieties to the exterior in an array of stacks, themselves stabilized through $\pi-\pi$ interactions.[15] Due to the intrinsic chirality of folic acid, the stacking is not parallel to the long axis of the columns (Scheme 1c−d). Structural studies conducted on folic acid and its derivatives have ascertained the chiral nature of pterin stacks and their mesophase behavior under different conditions.[16,17] The distance between pterin stacks has been determined by single crystal X-ray crystallography to be 3.28 and 3.4 Å in sodium folate solutions. The central cavity of the tetramer unit has been calculated, through conductance measurements of adsorbed cations, to be 3.7 Å.[18]

A costructure directing agent (CSDA), 3-aminopropyltriethoxysilane, is used to achieve charge matching between the anionically charged glutamate groups of folic acid (pK_a 8.3) and the hydrolysing and condensating silica fragments derived using the common precursor tetraethyl orthosilicate (TEOS). A variety of temperatures and reaction conditions were investigated to determine the most favorable synthetic approach. After a suitable reaction time, the synthesis gel was allowed to react hydrothermally at 100 °C to increase the degree of condensation of the silica network, as is typical for many mesoporous material syntheses. To obtain the mesoporous solid the FA template was removed by solvent extraction in an ethanol HCl solution followed by calcination at 500 °C under a flow of air.

Scheme 1

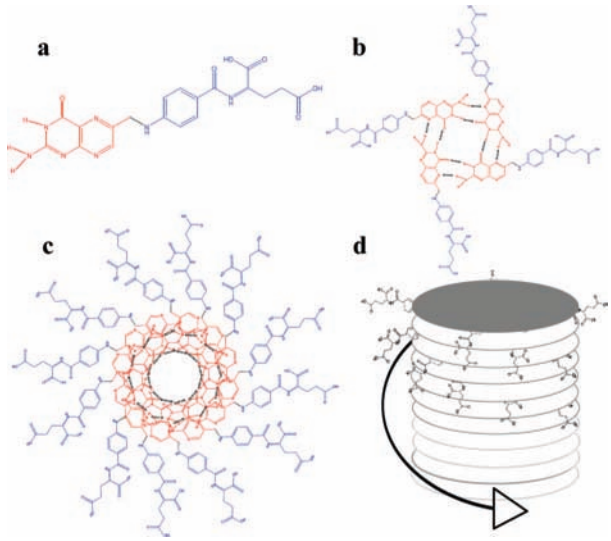

Figure 1 shows structural data derived from powder X-ray diffraction (XRD) on solid as-synthesized, extracted, and calcined samples with optimized molar ratios of FA/H_2O/APES/TEOS 0.13:230.5:0.33:1, respectively. This material is denoted from hereon NFM-1-G (Nanoporous Folic Acid Material-1-Gyroid). Low angle diffraction peaks can be indexed by a two-dimensional (2d-) hexagonal unit cell, *isostructural* with mesoporous material MCM-41 (p6 mm symmetry),[19] with unit cell parameter $a = 43.0$ Å for the as-synthesized sample and $a = 42.75$ and 40.9 Å for the extracted and calcined samples, respectively. Three peaks are typically observed at higher angles for as-synthesized samples; the broadest centered at 22° (2θ) is consistent with the amorphous nature of the silica wall, while the diffraction peak observed at 26.66° (2θ) can be associated with the stacking of pterin ($d = 3.36$ Å). The sharp peak at 44.30° 2θ ($d = 2.04$Å) in contrast with X-ray data obtained from folate solutions[20] indicates a lack of translational motion of the pterin stacks perpendicular to the *c*-axis of the hexagonal unit cell.

When samples were calcined directly after the synthesis, a reduction in the long-range mesoscale order was evident from XRD (data not shown). However, a solvent extraction treatment before calcination prevented the reduction in order, shown by the presence

[‡] Stockholm University.
[†] Uppsala University.

10.1021/ja8096477 CCC: $40.75

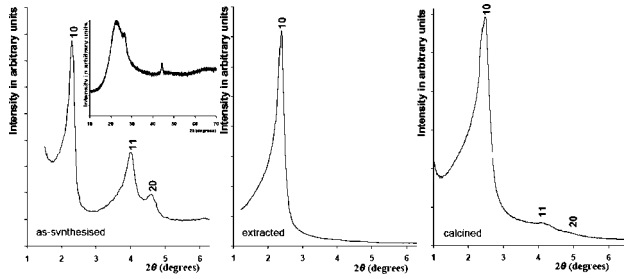

Figure 1. X-ray diffraction patterns of as-synthesized, extracted, and calcined mesoporous material NFM-1-G, templated by folic acid (FA). Inset shows an XRD pattern of as-synthesized sample recorded between 10° and 70° 2θ.

of high order reflections in the powder XRD pattern (11 and 20). An overall unit cell shrinkage of 2.1 Å was observed when solid as-synthesized samples were solvent extracted prior to calcination.

To derive textural data of NFM-1-G, nitrogen adsorption−desorption isotherms on extracted and calcined samples were measured and are shown in the Supporting Information. The isotherm curves are characterized by the absence of a hysteresis loop, typical of type IV (mesoporous isotherms). A pore filling step is observed at lower pressures: $p/p^o = 0.1-0.2$ for the extracted sample and $p/p^o = 0.2-0.3$ for the calcined samples. The absence of hysteresis in the desorption branch is due to the small size of the mesopores in these materials and the desorption branch closure point of nitrogen between $p/p^o = 0.37-0.42$ in relative pressure being above the pore diameter.[21] Pore size distributions reveal a low pore diameter for both extracted and calcined samples possessing sharp pore size distributions centered on 25 and 30 Å, respectively. A considerable increase in total pore volume is observed for calcined samples of NFM-1-G in comparison to extracted samples, with values of 0.59 and 0.33 cm^3/g, respectively. Likewise an increase in the surface area is also observed with a value of 1155 m^2/g for calcined NFM-1-G.

Solid state ^{29}Si NMR spectra of as-synthesized and calcined samples of NFM-1-G are shown in the Supporting Information. The presence of T^3 peaks in the as-synthesized sample confirms the incorporation of the amino silane within the mesoporous solid. The quota of organosilica to silica (T/Q) ratio is 0.24 and 0 for the as-synthesized and calcined samples, respectively. Surprisingly, the Q^3/Q^4 ratio in the as-synthesized material is smaller than that in the calcined sample, suggesting that a significant amount of T groups are converted to Q^3 upon calcination and that the quantity of Q^4 silica species remains largely unchanged during calcination. Furthermore, a small but significant amount of Q^2 species are observed in the spectrum of the calcined sample. The synthesis method comprises a hydrothermal step, which can contribute to further condense silicate species within the mesoporous wall. The ^{13}C NMR spectrum of the as-synthesized sample is additionally shown in the Supporting Information, confirming the presence of folic acid and aminopropyl moieties. The thermal decomposition of the FA template and the CSDA was followed by thermogravimetric analysis (TGA/DTG curves are show in the Supporting Information). Three distinct decomposition weight-loss regions can be observed. Region I (150−250 °C) is associated with the decomposition of freely grafted or surface bound organoalkoxysilane groups derived from the hydrolysis of APES, as has been observed previously in other syntheses employing CSDAs.[22] This broad peak is not present in extracted samples of NFM-1 samples. Region II (250−450 °C) can be associated with the overlapping decomposition of the organoalkoxysilane located within the internal surface and the glutamic acid component of the folic acid. Region III (450−800 °C) marks the decomposition of the pterin and *p*-amino benzoic acid. Generally these values occur at higher temperatures than those previously reported for the decomposition of free folic acid.[23] The amount of APES taking part in the supramolecular assembly of folic acid calculated from the TGA/DTG curves of extracted samples is 10.40 wt%. The total weight percentage of the FA template in the as-synthesized mesoporous material is hence calculated as 27.53 wt%. A comparison of infrared spectra (FTIR) recorded on folic acid and an as-synthesized sample of NFM-G-1 shows the disappearance of the O−H stretching bands of the terminal acid groups of folic acid in the as-synthesized sample. This is evidence of an interaction between these and the ammonium of the APES in the as-synthesized sample and, indeed, that the formation mechanism occurs via such a species.

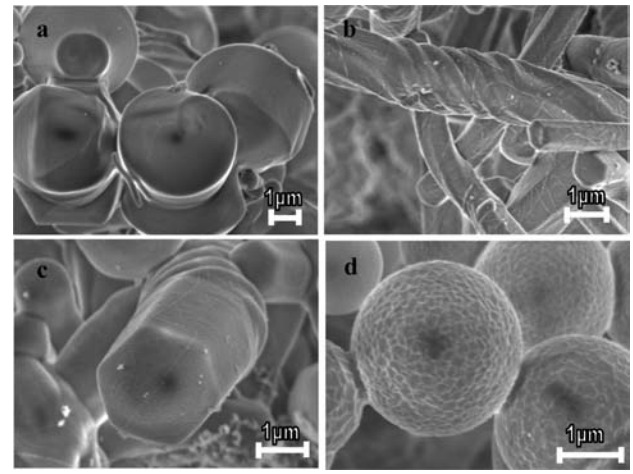

Figure 2. SEM images of calcined NFM-1 particles showing (a) gyroid particles of NFM-1-G and (b and c) chiral elongated particles NFM-1-R. (d) SEM image of NFM-1-S showing spherical particles.

SEM studies conducted on NFM-1 and related samples are shown in Figure 2. Sample NFM-1-G (Figure 2a) shows gyroid particles of 4 μm in size. Such morphologies have been obtained in preparations of mesoporous materials with hexagonal structures previously.[24] Small variations in reactant molar composition have led to various morphologies, with little or no variation in the XRD pattern of calcined samples (see Supporting Information). Addition of a higher amount of aminopropyl triethoxysilane leads to the formation of faceted hexagonal rod-type particles of diameters between 0.5 and 3 μm and lengths of between 5 and 20 μm (sample denoted NFM-1-R). Chiral motifs (Figure 2b,c) are clearly observed for short spacings of a few micrometers in length along the *c*-axis of particles. Although the chiral pitch is not homogeneous throughout the sample, only right-handed chiral twists could be observed on the basis of SEM investigations. A third morphology in the form of spheres 2−4 μm in diameter has additionally been obtained through variations in the amount of silica source TEOS (sample denoted NFM-1-S).

TEM images of calcined NFM-1-G samples and corresponding Fourier transformations (FT) are shown in Figure 3 and confirm the hexagonal structure, *p6mm* symmetry, with unit cell parameter $a = 39.30$ Å. TEM images recorded on calcined samples of NFM-1-R confirm the chiral nature of the pores shown in the Supporting Information. Images recorded on NFM-1-R clearly show fringes corresponding to the 10 planes (see Supporting Information).

Circular dichroism (CD) spectra recorded on solid samples of NFM-1-R (see Supporting Information) reveal that a chiral signature exists in the as-synthesized material. A positive peak with a maximum at 300 nm is observed arising from the chiral arrangement

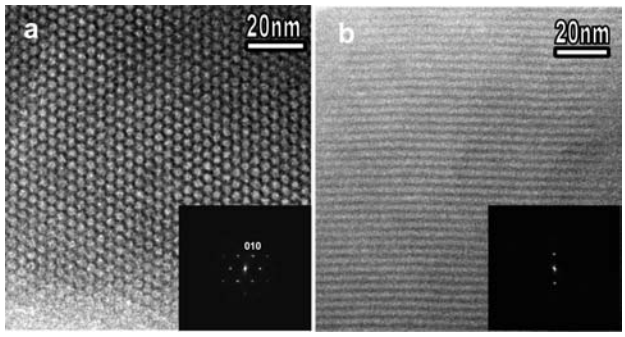

Figure 3. TEM images of calcined mesoporous NFM-1-G samples templated with folic acid, showing pores (a) parallel and (b) perpendicular to the hexagonal unit cell, respectively.

of tetrameric stacks within the folic acid template. The interpretation of these spectra is complex, and in general there is a shift toward higher wavelengths of maxima in the CD and absorption spectra when compared to spectra recorded on folic acid solutions at comparable concentrations and conditions. Overall, however, the data reveal that the formation mechanism taking place in this supramolecular templating approach is governed by the self-assembly of pterin stacks and electrostatic interactions between the negatively charged acid groups of the folic acid molecule and the ammonium of APES, and that hydrolysis and condensation take place around these chiral units. It is therefore expected that the propylamine groups on functionalized surfaces are also arranged in a similar chiral fashion, but whether this can be translated to advantages within applications in chiral separation or chiral catalysis remains to be proven. Preliminary release profile curves for NFM-1-R and NFM-1-S of FA performed in a phosphate buffer solution (pH = 7.4) indicate that a controlled release of the template is achieved over 24 h with a slight burst effect in the initial period measured (see Supporting Information).

In summary, a novel templating approach for ordered mesoporous materials with chiral hexagonal pore structures through the use of folic acid as the only pore forming agent has been presented. The materials are stable to calcination and possess high surface areas above 1000 m^2/g and pore sizes in the range 25−30 Å. Several other candidates containing pterin or guanosine groups are suitable for use as templates in the manner presented here, and we expect that further control of the pore geometry and structure will be accessible. Furthermore $\pi-\pi$ interactions with other drug molecules are envisaged and allow for a more efficient method of loading active substances within mesoporous materials. Our future work will concentrate on studying the synthetic versatility of this new approach and the application of these materials as delivery vehicles for folic acid together with anticancer drugs for targeted administration, which has recently been shown to be a potential anticancer therapeutic strategy.[25]

Acknowledgment. The authors would like to express their gratitude to Prof. Andreas Fischer (Royal Institute of Technology, Sweden) for access to XRD facilities as well as to Prof. Osamu Terasaki and Dr. Yasuhiro Sakamoto for many helpful discussions and access to their TEM facilities. A.E.G.B. is grateful for funding from Vetenskapsrådet (Junior Research Fellow). N.H. thanks the Vetenskapsrådet and the Berzelii Centre EXSELENT.

Supporting Information Available: A complete description of the materials and methods used in this study is included. Additionally nitrogen adsorption−desorption isotherms and ^{29}Si NMR MAS spectra measured on as synthesized and calcined samples of NFM-1-G as well as ^{13}C NMR are included. XRD patterns of as-synthesized samples of NFM-1-R (black) and NFM-1-S are shown. TGA/DTG curves of NFM-1-G, additional TEM and SEM data, and FTIR and circular dichroism spectra of as-synthesized NFM-1-R are included. This material is available free of charge via the Internet at http://pubs.acs.org.

References

(1) Cong, Y. S.; Wright, W. E.; Shay, J. W. *Microbiol. Mol. Biol. Rev.* **2002**, *66* (3), 407–425.
(2) Bacchi, C. J.; Nathan, H. C.; Hutner, S. H. *Science* **1980**, *210* (4467), 332–334.
(3) Choi, H.; Choi, S. R.; Zhou, R.; Kung, H. F.; Chen, I. W. *Acad. Radiol.* **2004**, *11* (9), 996–1004.
(4) Hong, S.; Leroueil, P. R.; Majoros, I. J.; Orr, B. G.; Baker, J. R.; Holl, M. M. B. *Chem. Biol.* **2007**, *14* (1), 105–113.
(5) Kresge, C. T.; Leonowicz, M. E.; Roth, W. J.; Vartuli, J. C.; Beck, J. S. *Nature* **1992**, *359* (6397), 710–712.
(6) Zhao, D.; Huo, Q.; Feng, J.; Chmelka, B. F.; Stucky, G. D. *J. Am. Chem. Soc.* **1998**, *120*, 6024.
(7) Sakamoto, Y.; Kaneda, M.; Terasaki, O.; Zhao, D. Y.; Kim, J. M.; Stucky, G.; Shim, H. J.; Ryoo, R. *Nature* **2000**, *408* (6811), 449–453.
(8) Che, S.; Garcia-Bennett, A. E.; Yokoi, T.; Sakamoto, K.; Kunieda, H.; Terasaki, O.; Tatsumi, T. *Nat. Mater.* **2003**, *2* (12), 801–805.
(9) Wan, Y.; Zhao, D. Y. *Chem. Rev.* **2007**, *107* (7), 2821–2860.
(10) Garcia-Bennett, A. E.; Lund, K.; Terasaki, O. *Angew. Chem., Int. Ed.* **2006**, *45* (15), 2434–2438.
(11) Wu, Y. Y.; Cheng, G. S.; Katsov, K.; Sides, S. W.; Wang, J. F.; Tang, J.; Fredrickson, G. H.; Moskovits, M.; Stucky, G. D. *Nat. Mater.* **2004**, *3* (11), 816–822.
(12) Che, S.; Liu, Z.; Ohsuna, T.; Sakamoto, K.; Terasaki, O.; Tatsumi, T. *Nature* **2004**, *429* (6989), 281–284.
(13) Xu, Y.; Cui, Y. X.; Jiang, D.; Wu, D.; Sun, Y. H. *Microporous Mesoporous Mater.* **2008**, *109* (1−3), 335–341.
(14) Balkus, K. J.; Scott, A. S.; Gimon-Kinsel, M. E.; Blanco, J. H. *Microporous Mesoporous Mater.* **2000**, *38* (1), 97–105.
(15) Davis, J. T.; Spada, G. P. *Chem. Soc. Rev.* **2007**, *36* (2), 296–313.
(16) Ciuchi, F.; Dinicola, G.; Franz, H.; Gottarelli, G.; Mariani, P.; Bossi, M. G. P.; Spada, G. P. *J. Am. Chem. Soc.* **1994**, *116* (16), 7064–7071.
(17) Bonazzi, S.; Demorais, M. M.; Gottarelli, G.; Mariani, P.; Spada, G. P. *Angew. Chem., Int. Ed. Engl.* **1993**, *32* (2), 248–250.
(18) Sakai, N.; Kamikawa, Y.; Nishii, M.; Matsuoka, T.; Kato, T.; Matile, S. *J. Am. Chem. Soc.* **2006**, *128* (7), 2218–2219.
(19) Beck, J. S.; Vartuli, J. C.; Roth, W. J.; Leonowicz, M. E.; Kresge, C. T.; Schmitt, K. D.; Chu, C. T.-W.; Olson, D. H.; Sheppard, E. W.; McCullen, S. B.; Higgins, J. B.; Schlenker, J. L. *J. Am. Chem. Soc.* **1992**, *114*, 10834.
(20) Giorgi, T.; Lena, S.; Mariani, P.; Cremonini, M. A; Masiero, S.; Pieraccini, S.; Rabe, J. P.; Samor, P.; Spada, G. P.; Gottarelli, G. *J. Am. Chem. Soc.* **2003**, *125*, 1474.
(21) Thommes, M.; Smarsly, B.; Groenewolt, M.; Ravikovitch, P. I.; Neimark, A. V. *Langmuir* **2006**, *22* (2), 756–764.
(22) Atluri, R.; Hedin, N.; Garcia-Bennett, A. E. *Chem. Mater.* **2008**, *20* (12), 3857–3866.
(23) Vora, A.; Riga, A.; Dollimore, D.; Alexander, K. *J. Therm. Anal. Calorim.* **2004**, *75* (3), 709–717.
(24) Yang, H.; Vovk, G.; Coombs, N.; Sokolov, I.; Ozin, G. A. *J. Mater. Chem.* **1998**, *8* (3), 743–750.
(25) Liong, M.; Lu, J.; Kovochich, M.; Xia, T.; Ruehm, S. G.; Nel, A. E.; Tamanoi, F.; Zink, J. I. *ACS Nano* **2008**, *2* (5), 889–896.

JA8096477